DOI: 10.1002/asia.201400131

FRET-Based Mitochondria-Targetable Dual-Excitation Ratiometric Fluorescent Probe for Monitoring Hydrogen Sulfide in Living Cells**

Lin Yuan*[a] and Qing-Ping Zuo[b]

Abstract: Hydrogen sulfide (H_2S) is connected with various physiological and pathological functions. However, understanding the important functions of H_2S remains challenging, in part because of the lack of tools for detecting endogenous H_2S. Herein, compounds **Ratio-H_2S 1/2** are the first FRET-based mitochondrial-targetable dual-excitation ratiometric fluorescent probes for H_2S on the basis of H_2S-promoted thiolysis of dinitrophenyl ether. With the enhancement of H_2S concentration, the excitation peak at $\lambda \approx 402$ nm of the phenolate form of the hydroxycoumarin unit drastically increases, whereas the excitation band centered at $\lambda \approx 570$ nm from rhodamine stays constant and can serve as a reference signal. Thus, the ratios of fluorescence intensities at $\lambda = 402$ and 570 nm (I_{402}/I_{570}) exhibit a drastic change from 0.048 in the absence of H_2S to 0.36 in the presence of 180 μM H_2S; this is a 7.5-fold variation in the excitation ratios. The favorable properties of the probe include the donor and acceptor excitation bands, which exhibit large excitation separations (up to 168 nm separation) and comparable excitation intensities, high sensitivity and selectivity, and function well at physiological pH. In addition, it is demonstrated that the probe can localize in the mitochondria and determine H_2S in living cells. It is expected that this strategy will lead to the development of a wide range of mitochondria-targetable dual-excitation ratiometric probes for other analytes with outstanding spectral features, including large separations between the excitation wavelengths and comparable excitation intensities.

Keywords: fluorescence · fluorescent probes · FRET · hydrogen sulfide · imaging agents

Introduction

Traditionally, hydrogen sulfide (H_2S) was only recognized as an environmental toxic gas with little or no physiological significance.[1] However, recent studies suggest that H_2S is a novel gaseous transmitter in cellular signaling pathways with the unique properties, in addition to nitric oxide (NO) and carbon monoxide (CO).[2] Endogenous levels of H_2S, which is endogenously produced in mitochondria by enzymes through metabolism,[2c] is involved in a vast number of physiological and pathological processes, such as regulation of vascular function, modulation of blood pressure, reduction of ischemia reperfusion injury, and protection of cells from oxidative stress and vascular injury.[1–5] Moreover, studies have shown that an abnormal H_2S level has also been associated with various diseases, including stroke, Alzheimer's disease, cardiovascular disease, Down's syndrome, diabetes, and liver cirrhosis.[6–9] In addition, H_2S is connected with various physiological and pathological functions; however, many of its underlying molecular events remain unknown. Therefore, selective detection of H_2S in living systems has received significant attention in recent years.

Recently, the construction of fluorescent probes for H_2S has attracted great attention.[10–12] However, the vast majority of them respond to H_2S with optical signal changes only in fluorescent intensity. In contrast to intensity-based fluorescent probes, ratiometric fluorescent probes, which display spectral shifts in the emission or excitation spectrum upon binding or interacting with the target analytes, can eliminate most or all environmental effects by self-calibration of two emission or excitation bands and can also increase the dynamic range of fluorescence measurement.[13,14] In addition, to be practically useful, probes should display two well-separated emission or excitation peaks with comparable intensities, which is highly desirable for determining the emission intensities and signal ratios with high accuracy and for enhancement of the dynamic range of signal ratios. To date, a few ratiometric fluorescent probes for monitoring H_2S in mitochondria have been reported,[11f–h] although they are highly desirable for biological imaging of H_2S in living cells.

Herein, we describe compounds **Ratio-H_2S 1/2** (Scheme 1) as new candidates for dual-excitation ratiometric fluorescent probes for H_2S. With the enhancement of H_2S concentration, the excitation peak at $\lambda \approx 402$ nm of the phenolate form of the hydroxycoumarin unit drastically increases, whereas the excitation band centered at $\lambda \approx 570$ nm from rhodamine stays constant and can serve as a reference

[a] Dr. L. Yuan
State Key Laboratory of Chemo/Biosensing and Chemometrics
College of Chemistry and Chemical Engineering
Hunan University, Changsha, Hunan 410082 (P.R. China)
E-mail: lyuan@hnu.edu.cn

[b] Q.-P. Zuo
Department of Pharmacy, The First Hospital of Changsha
Changsha, Hunan (P.R. China)

[**] FRET = Förster resonance energy transfer.

Supporting information for this article is available on the WWW under http://dx.doi.org/10.1002/asia.201400131.

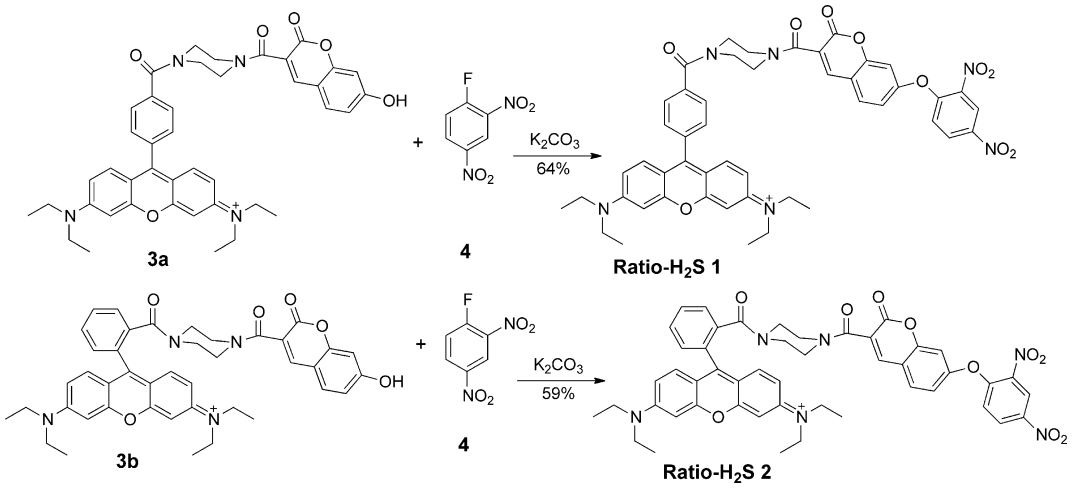

Scheme 1. Synthesis of the ratiometric fluorescence H_2S probes **Ratio-H_2S 1/2**.

signal. Thus, the ratios of fluorescence intensities at $\lambda = 402$ and 570 nm (I_{402}/I_{570}) exhibit a drastic change from 0.048 in the absence of H_2S to 0.36 in the presence of 180 μM H_2S, which is a 7.5-fold variation in the excitation ratios. The favorable properties of the probe include the donor and acceptor excitation bands, which exhibit large excitation separations (up to 168 nm separation) and comparable excitation intensities, high sensitivity and selectivity, and function well at physiological pH. In addition, we have demonstrated that the probe can localize in the mitochondria and be used for direct visualization of H_2S in living cells.

Results and Discussion

The rational design of the dual-excitation ratiometric fluorescent probes **Ratio-H_2S 1/2** is based on careful considerations. Recently, we introduced a Förster resonance energy transfer (FRET)-based molecular strategy (coumarin–rhodamine FRET platform) for the rational design of dual-excitation fluorescent probes with the two excitation bands, which showed large excitation separations and comparable excitation intensities.[15] Thus, coumarin–rhodamine FRET dyes are suitable as platforms for the development of dual-excitation ratiometric fluorescent probes. In this work, water-soluble coumarin–rhodamine FRET dyes **3a/b** with an optically tunable hydroxyl group were synthesized as the platform for the construction of new dual-excitation ratiometric fluorescent H_2S probes **Ratio-H_2S 1/2**. Furthermore, the H_2S-promoted thiolysis of dinitrophenyl ether was employed for the design of the probes **Ratio-H_2S 1/2**.[12e,f] Based on the structure–excitation property relationship of dyes **3a/b**,[15] we envisioned that probes **Ratio-H_2S 1/2** and dyes **3a/b** would display distinct excitation intensity profiles. This may serve as the basis for ratiometric fluorescence sensing of H_2S in living cells. The compounds **Ratio-H_2S 1/2** were readily prepared by reaction of compounds **3a/b** with 2,4-dinitrofluorobenzene under basic conditions in moderate yield (Scheme 1). ^1H and ^{13}C NMR spectroscopy and ESI-MS were employed to characterize the structures of the product.

With the probes **Ratio-H_2S 1/2** in hand, we evaluated the spectral properties in the absence or presence of H_2S in phosphate-buffered saline (PBS; pH 7.8, containing 5% EtOH, 3 mM cetyltrimethylammonium bromide (CTAB);[16] Figure 1 and Figures S1–S4 in the Supporting Information).

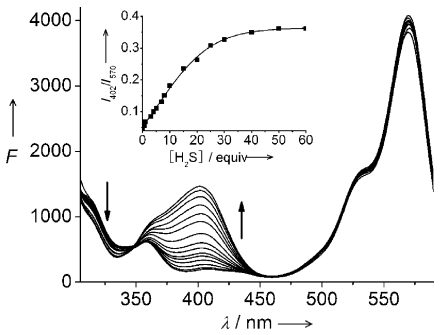

Figure 1. Fluorescence excitation spectral changes of **Ratio-H_2S 1** (3 μM) in the presence of increasing concentrations of NaHS (0–50 equiv) monitored at $\lambda = 590$ nm. The inset shows the ratiometric response (I_{402}/I_{570}) to varying concentrations of NaHS (0–60 equiv) monitored at $\lambda = 590$ nm. Each spectrum was acquired 30 min after H_2S addition at 25 °C.

Figure 1 shows the changes in the dual-excitation spectra of probe **Ratio-H_2S 1** to various H_2S concentrations, monitored at the rhodamine emission. The probe displayed a strong excitation band at $\lambda \approx 570$ nm and almost no excitation band at $\lambda \approx 402$ nm. Upon excitation of probe **Ratio-H_2S 1** at $\lambda =$ 402 nm, only a slight fluorescence emission band of rhodamine ($\lambda \approx 590$ nm) was observed (Figure S2 in the Supporting Information);, however, upon excitation of probe **Ratio-H_2S 1** at $\lambda = 560$ nm, a strong fluorescence emission at $\lambda \approx 590$ nm was observed (Figure S3 in the Supporting Information). Because the absorption and excitation wavelengths of the hydroxycoumarin moieties were blueshifted after alkylation, non-FRET was observed upon excitation at $\lambda =$

402 nm (Scheme S1 in the Supporting Information). With increased NaHS concentration, the excitation peak at $\lambda \approx 402$ nm, which was ascribed to the phenolate form of the hydroxycoumarin unit, was formed and gradually increased upon monitoring at $\lambda = 590$ nm. In addition, upon excitation at $\lambda = 402$ nm, the fluorescence emission band of rhodamine at $\lambda \approx 590$ nm gradually increased (Figure S2 in the Supporting Information). As the dinitrophenyl ether group in hydroxycoumarin moieties was deprotected and the absorbance at the excitation wavelength of the phenolate form of the hydroxycoumarin moieties increased (Figure S1 in the Supporting Information), FRET took place from hydroxycoumarin to rhodamine upon excitation at $\lambda = 402$ nm (Scheme S1 in the Supporting Information). In contrast, the excitation band centered at $\lambda \approx 570$ nm, which is attributed to the rhodamine moiety, is almost unchanged and can serve as a reference signal. Thus, the ratios of fluorescence intensities at $\lambda = 402$ and 570 nm (I_{402}/I_{570}) exhibited a drastic change from 0.048 in the absence of H_2S to 0.36 in the presence of 500 μM H_2S (Figure 1a), which was a 7.5-fold variation in the excitation ratios. In addition, probe **Ratio-H_2S 1** showed a good linearity between the ratios (I_{402}/I_{570}) and concentrations of NaHS in the range from 1 to 50 μM (Figure S4 in the Supporting Information) with a detection limit 0.5 μM (signal to noise (S/N) = 3).

The absorption changes of the probe in the presence of H_2S (Figure S1 in the Supporting Information) are in good agreement with the ratiometric response in the fluorescence excitation spectra. We confirmed that the product generated by the H_2S reaction with **Ratio-H_2S 1** was compound **3a** by MS analysis (Figure S5 in the Supporting Information), which was in accordance with the H_2S-promoted thiolysis of dinitrophenyl ether group.[12e,f] Similar H_2S-induced changes in the excitation spectra were also observed for probe **Ratio-H_2S 2** (Figure S6 in the Supporting Information).

The time course of the fluorescence excitation ratios of probe **Ratio-H_2S 1** at $\lambda = 402$ and 570 nm (I_{402}/I_{570}) in the absence or presence of H_2S is shown in Figure S7 in the Supporting Information. In the absence of H_2S, probe **Ratio-H_2S 1** exhibited no visible variations in the ratios of excitation intensities at $\lambda = 402$ and 570 nm ($I_{402}/I_{570} = 0.048$); this suggested that probe **Ratio-H_2S 1** was stable under the assay conditions and not converted into deprotected compound **3a**. However, upon addition of H_2S at room temperature, a marked increase in the ratio was observed within seconds, and the ratio essentially reached a maximum in 20 min, which was indicative of rapid deprotection of protected probe **Ratio-H_2S 1** to give deprotected compound **3a**, as anticipated. With a few exceptions,[10j,11g,j,12a] tens of minutes or hours are required for assays of many reported fluorescent H_2S probes; thus, probe **Ratio-H_2S 1** is faster or comparable with most reported fluorescent H_2S probes.[10–12] Because H_2S is a highly reactive species and poised to air oxidation, probe **Ratio-H_2S 1** can react with NaHS within seconds, which indicates that probe **Ratio-H_2S 1** may be able to trap H_2S in real biological systems. Kinetics measurements of the reaction of probe **Ratio-H_2S 1** (3 μM) with NaHS (200 μM) under pseudo-first-order conditions give an observed rate constant of $k_{obs} = 0.069\ min^{-1}$ (Figure S8 in the Supporting Information). In addition, the excitation ratio at $\lambda = 402$ and 570 nm (I_{402}/I_{570}) of probe **Ratio-H_2S 1** is stable over a pH region of 4–9 (Figure S8 in the Supporting Information). Upon the addition of sulfite, the excitation intensity ratio of probe **Ratio-H_2S 1** at I_{402}/I_{570} shows clear changes under different pH values from 5.5 to 9, and displays a clear response toward NaHS in the physiological pH region (7.0–8.0; Figure S9 in the Supporting Information). The results show that **Ratio-H_2S 1** is suitable for application under physiological conditions.

We further examined the selectivity of the probe **Ratio-H_2S 1/2**. As exhibited in Figure 2 and Figure S10 in the Supporting Information, the introduction of GSH (5 mM) and cysteine (0.5 mM) to probe **Ratio-H_2S 1** resulted in a slight

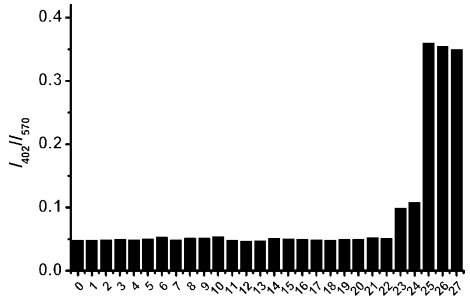

Figure 2. Fluorescence response of probe **Ratio-H_2S 1** (3 M) to various species (0.5 mM NO_2^-, N_3^-, HCO_3^-, K^+, Na^+, Ca^{2+}, Zn^{2+}, Mg^{2+}, Cl^-, Cys, F^-, Br^-, and I^-; 5 mM glutathione (GSH); 150 μM NaHS and other analytes tested) in PBS (pH 7.8, containing 5% EtOH and 3 mM CTAB). 0: free **Ratio-H_2S 1**; 1: HCO_3^-; 2: N_3^-; 3: ClO^-; 4: *t*BuOOH; 5: SO_3^{2-}; 6: $S_2O_3^{2-}$; 7: SCN^-; 8: NO_2^-; 9: H_2O_2; 10: NO; 11: O_2^-; 12: F^-; 13: Cl^-; 14: Br^-; 15: I^-; 16: lipoic acid; 17: Ca^{2+}; 18: Mg^{2+}; 19: Zn^{2+}; 20: K^+; 21: Na^+; 22: Fe^{3+}; 23: GSH; 24: Cys; 25: NaHS; 26: NaHS + GSH; 27: NaHS + Cys.

increase of the excitation ratio (I_{402}/I_{570}); however, H_2S induced a significant increase in the excitation ratio (I_{402}/I_{570}). In contrast, other biologically relevant analytes, RSS (lipoic acid, SO_3^{2-}, $S_2O_3^{2-}$, SCN^-), ROS/RNS (ClO^-, *t*BuOOH, NO_2^-, H_2O_2, NO, O_2^-), and metal ions and anions (Ca^{2+}, K^+, Na^+, Fe^{3+}, Zn^{2+}, Mg^{2+}, HCO_3^-, N_3^-, F^-, Cl^-, Br^-, and I^-), tested elicited no visible changes in the excitation ratio (I_{402}/I_{570}). In addition, probe **Ratio-H_2S 1** also displayed a large excitation ratio (I_{402}/I_{570}) response upon the addition of 150 μM NaHS in the presence of GSH (5 mM) or Cys (0.5 mM; Figure 2). Similar selectivity was also observed for probe **Ratio-H_2S 2** (Figure S11 in the Supporting Information). These data demonstrate that probes **Ratio-H_2S 1/2** have a high selectivity for H_2S over various biologically relevant analytes tested. In addition, probes **Ratio-H_2S 1/2** still display high selectivity for H_2S over thiols (Cys and GSH) in the absence of CTAB (Figure S12 in the Supporting Information).

The favorable fluorescence properties, appropriate amphipathicity, and low cytotoxicity (Figure S13 in the Supporting

Information) of probe **Ratio-H_2S 1** prompted us to test its potential use for H_2S ratiometric imaging in living cells. It was reported that positively charged dyes were inclined to localize in the mitochondria.[11g,h,17] In addition, H_2S was recently shown to be produced in mitochondria through metabolism.[2c] Therefore, it is necessary to investigate whether **Ratio-H_2S 1** can localize in the mitochondria. MCF-7 cells were simultaneously stained with probe **Ratio-H_2S 1** and MitoTracker Green at 37 °C for 20 min. The colocalization confirmed that probe **Ratio-H_2S 1** was mainly localized in the mitochondria of live cells (Figure 3).

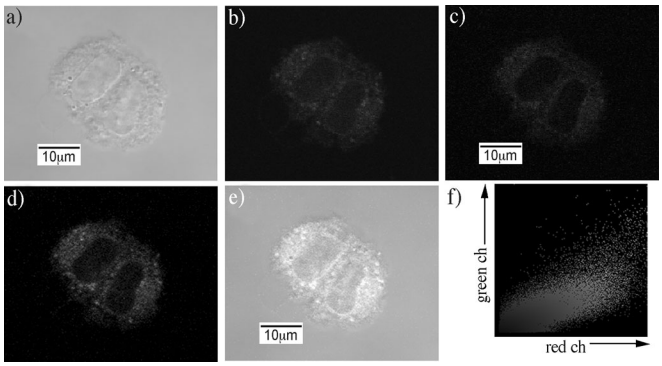

Figure 3. Bright field (a) and confocal fluorescence (b–c) images of MCF-7 cells. Cells were incubated with 3 μM **Ratio-H_2S 1** and 200 nM MitoTracker Green at 37 °C for 20 min in Dulbecco's modified Eagle medium (DMEM) media supplemented with 10% fetal bovine serum (FBS): b) MitoTracker Green with excitation at $\lambda = 488$ nm and a scan range of $\lambda = 520$–550 nm; c) probe **Ratio-H_2S 1** with excitation at $\lambda = 559$ nm and a scan range of $\lambda = 580$–650 nm; d) overlay of b) and c); e) overlay of a), b), and c); f) colocalization coefficient (Pearson's coefficient) of **Ratio-H_2S 1** and MitoTracker Blue of 0.90. Scale bar: 10 μm. (For a color version, see Figure S14 in the Supporting Information.)

To preliminarily illustrate the utility of the novel probes for fluorescence imaging in living cells, MCF-7 cells incubated with **Ratio-H_2S 1** for 10 min at 37 °C provide slight fluorescence (Figure 4b) when excited at $\lambda = 405$ nm. However, when the cells were pretreated with NaHS (100 μM) for 30 min and then further treated with **Ratio-H_2S 1**, there was a strong fluorescence (Figure 4e) when excited at $\lambda = 405$ nm. In contrast, when excited at $\lambda = 559$ nm, the brightness of the red fluorescence was almost unchanged in the absence or presence of H_2S (Figure 4c and f). These data are in good agreement with H_2S-induced variations of the emission intensity of probe **Ratio-H_2S 1**, as illustrated in Figures S2 and S3 in the Supporting Information. The ratiometric fluorescence images are shown in Figure S16 in the Supporting Information. Thus, the results indicate that probe **Ratio-H_2S 1** is cell membrane permeable and may be employed for ratiometric fluorescence imaging of H_2S in living cells.

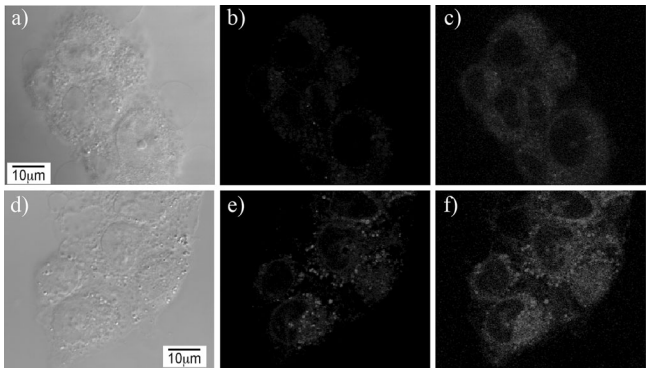

Figure 4. Bright-field and dual-excitation confocal fluorescence images of MCF-7 cells: a) bright-field image of MCF-7 cells only incubated with probe **Ratio-H_2S 1** (3 μM) for 10 min; b) fluorescence image of a) excited at $\lambda \approx 405$ nm and an emission scan range of $\lambda = 580$–650 nm; c) fluorescence image of a) excited at $\lambda \approx 559$ nm and an emission scan range of $\lambda = 580$–650 nm; d) bright-field image of MCF-7 cells pretreated with NaHS (100 μM) for 30 min at 37 °C, washed with PBS to remove the remaining NaHS, and further incubated with probe **Ratio-H_2S 1** (3 μM) for 10 min; e) fluorescence image of d) excited at $\lambda \approx 405$ nm and an emission scan range of $\lambda = 580$–650 nm; f) fluorescence image of d) excited at $\lambda \approx 559$ nm and an emission scan range of $\lambda = 580$–650 nm. Scale bar: 10 μm. (For a color version, see Figure S15 in the Supporting Information.)

Conclusions

We developed **Ratio-H_2S 1/2** as the first FRET-based dual-excitation ratiometric fluorescent probes for H_2S. Upon addition of H_2S, the excitation band at $\lambda \approx 402$ nm of the hydroxycoumarin unit drastically increased, whereas the excitation band centered at $\lambda \approx 570$ nm from rhodamine stayed constant and served as a reference signal; thus resulting in the ratiometric detection of H_2S. Favorable properties of the probe include the donor and acceptor excitation bands, which exhibited large excitation separations and comparable excitation intensities, high sensitivity and selectivity. In addition, we demonstrated that the probe could localize in the mitochondria and determined H_2S in living cells. It is expected that this strategy will lead to the development of a wide range of mitochondria-targetable dual-excitation ratiometric probes for other analytes with outstanding spectral features, including large separations between the excitation wavelengths and comparable excitation intensities.

Experimental Section

Materials and Instruments

Unless otherwise stated, all reagents were purchased from commercial suppliers and used without further purification. Solvents were purified by standard methods prior to use. Low-resolution mass spectra were performed by using an LCQ Advantage ion trap mass spectrometer from Thermo Finnigan or Agilent 1100 HPLC/MSD spectrometer. High-resolution mass spectrometry (HRMS) analyses were performed on a Finnigan MAT 95 XP spectrometer. NMR spectra were recorded on an INOVA-400 spectrometer, with tetramethylsilane (TMS) as an internal standard. Electronic absorption spectra were obtained on a LabTech UV

Power spectrometer. Photoluminescent spectra were recorded with a HITACHI F4600 fluorescence spectrophotometer. Imaging of the cells was performed with an Olympus FV1000 confocal microscope. The pH measurements were performed on a Mettler-Toledo Delta 320 pH meter. TLC analyses were performed on silica gel plates and column chromatography was conducted over silica gel (mesh 200–300), both of which were obtained from Qingdao Ocean Chemicals.

Synthesis of ***Ratio-H_2S 1/2***

Compound **4** (44.5 mg, 0.24 mmol) and Cs_2CO_3 (78.6 mg, 0.24 mmol) were added to a solution of **3a/b** (108.0 mg, 0.12 mmol) in anhydrous CH_2Cl_2 (6 mL) at room temperature, and then the reaction mixture was stirred at room temperature for 6 h under a nitrogen atmosphere. The solvent was removed under reduced pressure and the resulting residue was subjected to column chromatography on silica (CH_2Cl_2 to CH_2Cl_2/CH_3OH = 9: 1) to yield **Ratio-H_2S 1/2** as a red powder.

Ratio-H_2S 1: Yield: 69 mg, 64%; ^{1}H NMR (400 MHz, CD_3OD): δ = 1.25 (t, J = 6.8 Hz, 12H), 3.50-3.83 (16H), 6.92 (s, 2H), 7.01 (2H), 7.13 (d, J = 7.6 Hz, 1H), 7.14 (s, 1H), 7.35 (2H), 7.38 (d, J = 9.2 Hz, 1H), 7.52–7.54 (2H), 7.69–7.71 (2H), 7.77 (d, J = 9.2 Hz, 1H), 8.12 (s, 1H), 8.45 (dd, J = 9.2, 2.4 Hz, 1H), 8.85 ppm (d, J = 2.4 Hz, 1H); ^{13}C NMR (100 MHz, CD_3OD): δ = 13.8, 24.7, 31.7, 47.9, 44.2, 98.5, 109.1, 115.4, 116.6, 118.3, 124.1, 124.2, 125.4, 129.8, 131.5, 132.2, 133.4, 133.9, 136.4, 139.3, 143.3, 145.4, 145.8, 155.6, 157.9, 158.2, 158.6, 160.5, 161.1, 166.9, 172.7 ppm; MS (ESI): 865.3 $[M]^+$; HRMS (ESI): m/z calcd for $C_{48}H_{45}N_6O_{10}^+$ $[M]^+$: 865.3192; found: 865.3197.

Ratio-H_2S 2: Yield: 64 mg, 59; ^{1}H NMR (400 MHz, CD_3OD): δ = 1.24 (t, J = 7.2 Hz, 12H), 3.18 (1H), 3.33-3.55 (7H), 3.63 (q, J = 7.2 Hz, 12H), 6.91 (2H), 6.98–7.03 (2H), 7.12 (s, 2H), 7.18–7.25 (2H), 7.38 (t, J = 8.4 Hz, 1H), 7.46 (s, 1H), 7.62–7.72 (4H), 8.04 (d, J = 7.6 Hz, 1H), 8.45 (t, J = 7.2 Hz, 1H), 8.85 ppm (s, 1H); ^{13}C NMR (100 MHz, CD_3OD): δ = 13.9, 24.0, 43.7, 47.9, 98.4, 109.0, 115.8, 116.5, 118.1, 118.2, 124.1, 125.2, 130.0, 131.5, 132.4, 132.8, 133.4, 134.2, 137.5, 143.3, 145.3, 145.9, 155.6, 157.9, 158.2, 161.2, 166.7, 170.6 ppm; MS (ESI): 865.3 $[M]^+$; HRMS (ESI): m/z calcd for $C_{48}H_{45}N_6O_{10}^+$ $[M]^+$: 865.3192; found: 865.3186.

MCF-7 Cell Culture and Imaging

MCF-7 cells were obtained from Xiangya Hospital and cultured in DMEM supplemented with 10% FBS in an atmosphere of 5% CO_2 and 95% air at 37 °C. For imaging studies, the cells were plated and allowed to adhere for 24 h. Immediately before the experiments, the cells were washed with PBS, followed by incubation with probe **Ratio-H_2S 1** (3 μM) for 10 min at 37 °C (in PBS containing 0.5% EtOH). For intracellular H_2S imaging, the cells were incubated with NaHS (100 μM) in PBS at 37 °C for 30 min. After removal of excess NaHS and washing with PBS, the cells were incubated with probe **Ratio-H_2S 1** (3 μM) for 10 min at 37 °C (in PBS containing 0.5% EtOH). Cell imaging was performed after washing the cells three times with PBS.

Cytotoxicity Assays

MCF-7 cells were cultured in DMEM containing 10% FBS supplemented with 100 U mL^{-1} of penicillin and 100 μg mL^{-1} streptomycin in an atmosphere of 5% CO_2 and 95% air at 37 °C. The cells were seeded into 96-well plates and then 1.0, 2.0, 5.0, 10.0, or 15.0 μM (final concentration) of **Ratio-H_2S 1** (99.9% DMEM and 0.1% DMSO) was added (n = 6). Subsequently, the cells were incubated at 37 °C in an atmosphere of 5% CO_2 and 95% air for 24 h. An untreated assay with DMEM (n = 6) was also performed under the same conditions.

Acknowledgements

This work was financially supported by the NSFC (21302050), the Hunan Provincial Natural Science Foundation of China (grant no. 14JJ2047), and the Young Teachers' Growth Plan of Hunan University.

[1] a) D. R. Linden, J. Furne, G. J. Stoltz, M. S. Abdel-Rehim, M. D. Levitt, J. H. Szurszewski, *Br. J. Pharmacol.* **2012**, *165*, 2178–2190; b) R. G. Hendrickson, A. Chang, R. J. Hamilton, *Am. J. Ind. Med.* **2004**, *45*, 346–350; c) R. J. Reiffenstein, W. C. Hulbert, S. H. Roth, *Annu. Rev. Pharmacol. Toxicol.* **1992**, *32*, 109–134.

[2] a) C. E. Paulsen, K. S. Carroll, *Chem. Rev.* **2013**, *113*, 4633–4679; b) K. Kashfi, K. R. Olson, *Biochem. Pharmacol.* **2013**, *85*, 689–703; c) M. Fu, W. Zhang, L. Wu, G. Yang, H. Li, R. Wang, *Proc. Natl. Acad. Sci. USA* **2012**, *109*, 2943–2948; d) L. Li, P. Rose, P. K. Moore, *Annu. Rev. Pharmacol. Toxicol.* **2011**, *51*, 169–187; e) K. Shatalin, E. Shatalina, A. Mironov, E. Nudler, *Science* **2011**, *334*, 986–990; f) E. Lowicka, J. Beltowski, *Pharmacol. Rep.* **2007**, *59*, 4–24.

[3] a) O. Kabil, R. Banerjee, *J. Biol. Chem.* **2010**, *285*, 21903–21907; b) E. Streeter, H. H. Ng, J. L. Hart, *Med. Gas Res.* **2013**, *3*, 9, DOI: 10.1186/2045-9912-3-9.

[4] G. Yang, L. Wu, B. Jiang, W. Yang, J. Qi, K. Cao, Q. Meng, A. K. Mustafa, W. Mu, S. Zhang, S. H. Snyder, R. Wang, *Science* **2008**, *322*, 587–590.

[5] R. C. O. Zanardo, V. Brancaleone, E. Distrutti, S. Fiorucci, G. Cirino, J. L. Wallace, *FASEB J.* **2006**, *20*, 2118–2120.

[6] a) Y. Ogasawara, S. Isoda, S. Tanabe, *Biol. Pharm. Bull.* **1994**, *17*, 1535–1542; b) P. Nagy, C. C. Winterbourn, *Chem. Res. Toxicol.* **2010**, *23*, 1541–1543.

[7] K. Eto, T. Asada, K. Arima, T. Makifuchi, H. Kimura, *Biochem. Biophys. Res. Commun.* **2002**, *293*, 1485–1488.

[8] a) P. Kamoun, M.-C. Belardinelli, A. Chabli, K. Lallouchi, B. Chadefaux-Vekemans, *Am. J. Med. Genet. A* **2003**, *116A*, 310–311; b) W. Yang, G. Yang, X. Jia, L. Wu, R. Wang, *J. Physiol.* **2005**, *569*, 519–531.

[9] K. Qu, C. P. Chen, B. Halliwell, P. K. Moore, P. T. Wong, *Stroke* **2006**, *37*, 889–893.

[10] For some examples, see: a) A. R. Lippert, E. J. New, C. J. Chang, *J. Am. Chem. Soc.* **2011**, *133*, 10078–10080; b) H. Zhang, P. Wang, G. Chen, H.-Y. Cheung, H. Sun, *Tetrahedron Lett.* **2013**, *54*, 4826–4829; c) L. A. Montoya, M. D. Pluth, *Chem. Commun.* **2012**, *48*, 4767–4769; d) B. Chen, C. Lv, X. Tang, *Anal. Bioanal. Chem.* **2012**, *404*, 1919–1923; e) G. Zhou, H. Wang, Y. Ma, X. Chen, *Tetrahedron* **2013**, *69*, 867–870; f) S. K. Das, C. S. Lim, S. Y. Yang, J. H. Han, B. R. Cho, *Chem. Commun.* **2012**, *48*, 8395–8397; g) Z. Wu, Z. Li, L. Yang, J. Han, S. Han, *Chem. Commun.* **2012**, *48*, 10120–10122; h) W. Li, W. Sun, X. Yu, L. Du, M. Li, *J. Fluoresc.* **2013**, *23*, 181–186; i) Q. Wan, Y. Song, Z. Li, X. Gao, H. Ma, *Chem. Commun.* **2013**, *49*, 502–504; j) H. Peng, Y. Cheng, C. Dai, A. L. King, B. L. Predmore, D. J. Lefer, B. Wang, *Angew. Chem.* **2011**, *123*, 9846–9849; *Angew. Chem. Int. Ed.* **2011**, *50*, 9672–9675.

[11] For *some* examples, see: a) C. Liu, J. Pan, S. Li, Y. Zhao, L. Y. Wu, C. E. Berkman, A. R. Whorton, M. Xian, *Angew. Chem.* **2011**, *123*, 10511–10513; *Angew. Chem. Int. Ed.* **2011**, *50*, 10327–10329; b) Z. Xu, L. Xu, J. Zhou, Y. Xu, W. Zhu, X. Qian, *Chem. Commun.* **2012**, *48*, 10871–10873; c) Y. Qian, J. Karpus, O. Kabil, S.-Y. Zhang, H.-L. Zhu, R. Banerjee, J. Zhao, C. He, *Nat. Commun.* **2011**, *2*, 495; d) X. Chen, S. Wu, J. Han, S. Han, *Bioorg. Med. Chem. Lett.* **2013**, *23*, 5295–5299; e) X. Li, S. Zhang, J. Cao, N. Xie, T. Liu, B. Yang, Q. He, Y. Hu, *Chem. Commun.* **2013**, *49*, 8656–8658; f) S. K. Bae, C. H. Heo, D. J. Choi, D. Sen, E.-H. Joe, B. R. Cho, H. M. Kim, *J. Am. Chem. Soc.* **2013**, *135*, 9915–9923; g) Y. Chen, C. Zhu, Z. Yang, J. Chen, Y. He, Y. Jiao, W. He, L. Qiu, J. Cen, Z. Guo, *Angew. Chem.* **2013**, *125*, 1732–1735; *Angew. Chem. Int. Ed.* **2013**, *52*, 1688–1691; h) X. Wang, J. Sun, W. Zhang, X. Ma, J. Lv, B. Tang, *Chem. Sci.* **2013**, *4*, 2551–2556; i) M.-Y. Wu, K. Li, J.-T. Hou, Z. Huang, X.-Q. Yu, *Org. Biomol. Chem.* **2012**, *10*, 8342–8347; j) J. Liu, Y.-Q. Sun, J. Zhang, T. Yang, J. Cao, L. Zhang, W. Guo, *Chem. Eur. J.* **2013**, *19*, 4717–4722; k) Q. Huang, X.-F. Yang, H. Li, *Dyes Pigm.* **2013**, *99*, 871–877.

[12] For some examples, see: a) K. Sasakura, K. Hanaoka, N. Shibuya, Y. Mikami, Y. Kimura, T. Komatsu, T. Ueno, T. Terai, H. Kimura, T. Nagano, *J. Am. Chem. Soc.* **2011**, *133*, 18003–18005; b) F. Hou, L. Huang, P. Xi, J. Cheng, X. Zhao, G. Xie, Y. Shi, F. Cheng, X. Yao,

D. Bai, Z. Zeng, *Inorg. Chem.* **2012**, *51*, 2454–2560; c) X. Wu, H. Li, Y. Kan, B. Yin, *Dalton Trans.* **2013**, *42*, 16302–16310; d) J.-T. Hou, B.-Y. Liu, K. Li, K.-K. Yu, M.-B. Wu, X.-Q. Yu, *Talanta* **2013**, *116*, 434–440; e) T. Liu, X. Zhang, Q. Qiao, C. Zou, L. Feng, J. Cui, Z. Xu, *Dyes Pigm.* **2013**, *99*, 537–542; f) L. Yuan, Q.-P. Zuo, *Sens. Actuators B* **2014**, *96*, 151–155; g) C. Yu, X. Li, F. Zeng, F. Zheng, S. Wu, *Chem. Commun.* **2013**, *49*, 403–405.

[13] J. P. Y. Kao, A. T. Harootunian, R. Y. Tsien, *J. Biol. Chem.* **1989**, *264*, 8171–8178.

[14] a) X. Zhang, Y. Xiao, X. Qian, *Angew. Chem.* **2008**, *120*, 8145–8149; *Angew. Chem. Int. Ed.* **2008**, *47*, 8025–8029; b) L. Long, L. Zhou, L. Wang, S. Meng, A. Gong, F. Du, C. Zhang, *Anal. Methods* **2013**, *5*, 6605–6610; c) A. P. Demchenko, *Introduction to Fluorescence Sensing*, Springer, New York, **2008**, pp. 102–104.

[15] L. Yuan, W. Lin, Z. Cao, J. Wang, B. Chen, *Chem. Eur. J.* **2012**, *18*, 1247–1255.

[16] CTAB micelles were reported to accelerate the reaction between the sulfide anion and the probe, which may be attributed to CTAB increasing the solubility of the probe in aqueous buffers and also absorbing sulfide anions, see: a) Y. Liu, G. Feng, *Org. Biomol. Chem.* **2014**, *12*, 438–445; b) B. Peng, W. Chen, C. Liu, E. W. Rosser, A. Pacheco, Y. Zhao, H. C. Aguilar, M. Xian, *Chem. Eur. J.* **2014**, *20*, 1010–1016.

[17] For some examples, see: a) S. Wu, Y. Song, Z. Li, Z. Wu, J. Han, S. Han, *Anal. Methods* **2012**, *4*, 1699–1703; b) Y. Koide, Y. Urano, S. Kenmoku, H. Kojima, T. Nagano, *J. Am. Chem. Soc.* **2007**, *129*, 10324–10325; c) S. L. Sensi, D. Ton-That, J. H. Weiss, A. Rothe, K. R. Gee, *Cell Calcium* **2003**, *34*, 281–284; d) F. Liu, T. Wu, J. Cao, H. Zhang, M. Hu, S. Sun, F. Song, J. Fan, J. Wang, X. Peng, *Analyst* **2013**, *138*, 775–778; e) K. Xu, L. Wang, M. Qiang, L. Wang, P. Li, B. Tang, *Chem. Commun.* **2011**, *47*, 7386–7388.

Received: January 28, 2014
Revised: February 17, 2014
Published online: April 1, 2014

